



Effects of metallicity, star-formation conditions, and evolution in B and Be stars. II: Small Magellanic Cloud, field of NGC 330.

Christophe Martayan, Yves Frémat, Anne-Marie Hubert, Michele Floquet,
Jean Zorec, Coralie Neiner

► To cite this version:

Christophe Martayan, Yves Frémat, Anne-Marie Hubert, Michele Floquet, Jean Zorec, et al.. Effects of metallicity, star-formation conditions, and evolution in B and Be stars. II: Small Magellanic Cloud, field of NGC 330.. 2006. hal-00098275

HAL Id: hal-00098275

<https://hal.science/hal-00098275>

Preprint submitted on 25 Sep 2006

HAL is a multi-disciplinary open access archive for the deposit and dissemination of scientific research documents, whether they are published or not. The documents may come from teaching and research institutions in France or abroad, or from public or private research centers.

L'archive ouverte pluridisciplinaire **HAL**, est destinée au dépôt et à la diffusion de documents scientifiques de niveau recherche, publiés ou non, émanant des établissements d'enseignement et de recherche français ou étrangers, des laboratoires publics ou privés.

Effects of metallicity, star-formation conditions, and evolution in B and Be stars.

II: Small Magellanic Cloud, field of NGC 330.

C. Martayan¹, Y. Frémat², A.-M. Hubert¹, M. Floquet¹, J. Zorec³, and C. Neiner¹

¹ GEPI, UMR 8111 du CNRS, Observatoire de Paris-Meudon, 92195 Meudon Cedex, France

² Royal Observatory of Belgium, 3 avenue circulaire, 1180 Brussels, Belgium

³ Institut d'Astrophysique de Paris (IAP), 98bis boulevard Arago, 75014 Paris, France

Received /Accepted

ABSTRACT

Aims. We search for effects of metallicity on B and Be stars in the Small and Large Magellanic Clouds (SMC and LMC) and in the Milky Way (MW). We extend our previous analysis of B and Be stars populations in the LMC to the SMC. The rotational velocities of massive stars and the evolutionary status of Be stars are examined with respect to their environments.

Methods. Spectroscopic observations of hot stars belonging to the young cluster SMC-NGC 330 and its surrounding region have been obtained with the VLT-GIRAFFE facilities in MEDUSA mode. We determine fundamental parameters for B and Be stars with the GIRFIT code, taking into account the effect of fast rotation, and the age of observed clusters. We compare the mean $V \sin i$ obtained by spectral type- and mass-selection for field and cluster B and Be stars in the SMC with the one in the LMC and MW.

Results. We find that (i) B and Be stars rotate faster in the SMC than in the LMC, and in the LMC than in the MW; (ii) at a given metallicity, Be stars begin their main sequence life with a higher initial rotational velocity than B stars. Consequently, only a fraction of B stars that reach the ZAMS with a sufficiently high initial rotational velocity can become Be stars; (iii) the distributions of initial rotational velocities at the ZAMS for Be stars in the SMC, LMC and MW are mass- and metallicity-dependent; (iv) the angular velocities of B and Be stars are higher in the SMC than in the LMC and MW; (v) in the SMC and LMC, massive Be stars appear in the second part of the main sequence, contrary to massive Be stars in the MW.

Key words. Stars: early-type – Stars: emission-line, Be – Galaxies: Magellanic Clouds – Stars: fundamental parameters – Stars: evolution – Stars: rotation

1. Introduction

The origin of the Be phenomenon has given rise to long debates. Whether it is linked to stellar evolution or initial formation conditions remains a major issue. Thus, finding out differences in the physical properties of B and Be stars populations belonging to environments with different metallicity could provide new clues to understand the Be phenomenon.

To investigate the influence of metallicity, star-formation conditions and stellar evolution on the Be phenomenon, we have undertaken an exhaustive study of B and Be stars belonging to young clusters or field of the Small and Large Magellanic Clouds (SMC and LMC), because these galaxies have a lower metallicity than the Milky Way (MW). For this purpose we made use of the new FLAMES-GIRAFFE instru-

mentation installed at the VLT-UT2 at ESO, which is particularly well suited, in MEDUSA mode, to obtain high quality spectra of large samples needed for the study of stellar populations. In Martayan et al. (2006a, hereafter M06), we reported on the identification of 177 B and Be stars belonging to the young cluster LMC-NGC 2004 and its surrounding region. In Martayan et al. (2006b, hereafter Paper I), we determined fundamental parameters of a large fraction of the sample in the LMC, taking into account rotational effects (stellar flattening, gravitational darkening) when appropriate. We then investigated the effects of metallicity on rotational velocities. We concluded that Be stars begin their life on the main sequence (MS) with a higher initial velocity than B stars. Moreover, this initial velocity is sensitive to the metallicity. Consequently, only a fraction of the B stars that reach the ZAMS with a sufficiently high initial rotational velocity can become Be stars. However,

Send offprint requests to: C. Martayan

Correspondence to: christophe.martayan@obspm.fr

ccsd-00098275, version 1 - 25 Sep 2006

no clear influence of metallicity on the rotational velocity of B stars was found.

The present paper deals with a large sample of B and Be stars in the SMC, which has a lower metallicity than the LMC. With the determination of fundamental parameters, and the study of the evolutionary status and abundances, we aim at confirming and enlarging our results derived from the study of B and Be stars in Martayan et al. (2005a) and from the LMC (Paper I).

2. Observations

This work makes use of spectra obtained with the multifibre VLT-FLAMES/GIRAFFE spectrograph in Medusa mode (131 fibres) at medium resolution ($R=6400$) in setup LR02 (396.4 - 456.7 nm). Observations (ESO runs 72.D-0245A and 72.D-0245C) were carried out in the young cluster SMC-NGC 330 and in its surrounding field, as part of the Guaranteed Time Observation programmes of the Paris Observatory (P.I.: F. Hammer). The observed fields (25' in diameter) are centered at $\alpha(2000) = 00^h 55^m 15^s$, $\delta(2000) = -72^\circ 20' 00''$ and $\alpha(2000) = 00^h 55^m 25^s$, $\delta(2000) = -72^\circ 23' 30''$. Besides the young cluster NGC 330, this field contains several high-density groups of stars (NGC306, NGC299, OGLE-SMC99, OGLE-SMC109, H86 145, H86 170, Association [BS95]78, Association SMC ASS39). Note that we corrected the coordinates of NGC299 given in Simbad (CDS) with EIS coordinates (Momany et al. 2001). Spectra have been obtained on October 21, 22, and 23, 2003 and September 9 and 10, 2004; at those dates, the heliocentric velocity is respectively 7 and 12 km s^{-1} . The strategy and conditions of observations, as well as the spectra reduction procedure, are described in M06. A sample of 346 stars has been observed within the two observing runs. Since the V magnitude of the selected targets ranges from 13.5 to 18.8 mag, the integration time varied between 1h and 2h. However, as the seeing was not optimal during the first run, the S/N ratio is only about 50 on average, with individual values ranging from 20 to 130.

We pre-selected 11544 B-type star candidates with $14 \leq V \leq 18$ and a colour index $B-V < 0.35$, among the 192437 stars listed in the EIS SMC5 field by the EIS team (Momany et al. 2001), keeping in mind the intrinsic value $E(B-V)=0.08$ (Keller et al. 1999) for the SMC. We then observed three fields with VLT-FLAMES/GIRAFFE. Since for each field maximum 130 stars can be observed, we collected data for 346 objects among the 5470 B-type star candidates located in these fields for the selected magnitude range. The ratio of observed to observable B-type stars in the GIRAFFE fields is thus 6.3%. This represents a statistically significant sample. From the observations we confirm the B spectral type for 333 of the 346 stars. Of the remaining 13 objects, 4 are O stars, 6 are A stars, 1 is a cold supergiant, 1 is a planetary nebula, and 1 is a HB[e]. The 333 B-type objects further include 131 Be stars.

The V versus B-V colour diagram (Fig. 1), derived from EIS photometry (Momany et al. 2001), shows the O, B, A and Be stars in our sample compared to all the stars in the EIS-SMC 5 field.

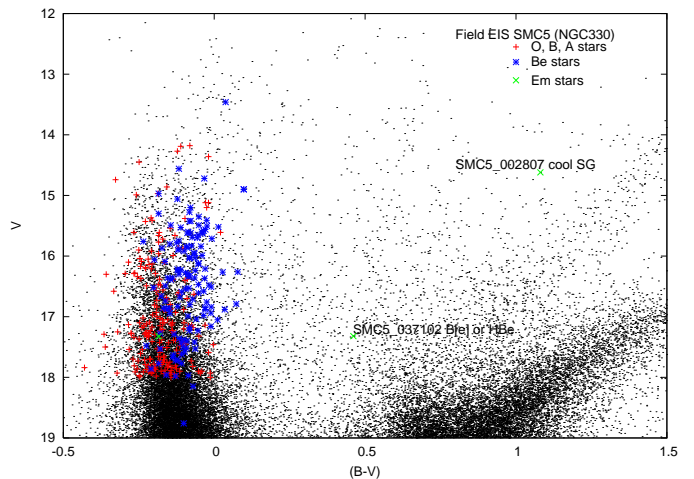


Fig. 1. V versus (B-V) colour diagram from EIS photometry in the EIS SMC 5 field. The ' ' symbols correspond to all stars in this field. '*' show the Be stars, '+' the O-B-A stars and 'x' the other emission-line stars in the sample.

3. Determination of fundamental parameters

As in Paper I we make use of the GIRFIT least-square procedure (Frémat et al. 2006) to derive the fundamental parameters: effective temperature (T_{eff}), surface gravity ($\log g$), projected rotational velocity ($V \sin i$) and radial velocity (RV). This procedure fits the observations with theoretical spectra interpolated in a grid of stellar fluxes computed with the SYNSPEC programme and from model atmospheres calculated with TLUSTY (Hubeny & Lanz 1995, see references therein) or/and with ATLAS9 (Kurucz 1993; Castelli et al. 1997). The grid of model atmospheres we use to build the GIRFIT input of stellar fluxes is obtained in the same way as in our LMC study, but for the metallicity of the SMC.

The metallicities of the model atmospheres are chosen to be as close as possible to the NGC 330 average value, $[m/H] = -0.6$ (where $[m/H] = \log(m/H)_{\text{SMC}} - \log(m/H)_{\odot}$), estimated from Jasiewicz & Thévenin (1994). The Kurucz and OSTAR 2002 models we use are therefore those calculated with a $[m/H]$ close to -0.6. Finally, the complete input flux grid is built assuming the averaged element abundances derived by Jasiewicz & Thévenin (1994) for C, Mg, Ca, Ti, Cr, Mn and Fe. The other elements, except hydrogen and helium, are assumed to be underabundant by -0.6 dex relative to the Sun.

It is worth noting that GIRFIT does not include the effects of fast rotation. Therefore, for rapidly rotating stars, we need to correct the stellar parameters with the FASTROT computer code (Frémat et al. 2005) assuming a solid-body-type rotation. We then obtain the 'parent non-rotating counterpart' (pnrc; see Frémat et al. 2005) stellar parameters (T_{eff}^0 , $\log g_0$, $V \sin i^{\text{true}}$) for a given Ω/Ω_c .

For a more detailed description of the grid of model atmospheres we use, the fitting criteria we adopt in the GIRFIT procedure, and the correction for fast rotation we apply on fundamental parameters of Be stars, we refer the reader to Paper I (Sect. 3).

Finally, we determine the spectral classification of each star with two methods. The calibration we establish to estimate these spectral types is described in Paper I. The agreement between the two methods is not as good as for the stars observed in the LMC (Paper I), because the observations for the SMC have a lower S/N ratio.

4. Stellar parameters of the sample stars

In this section we present the stellar parameters and spectral classification we obtained for O-B-A and Be stars.

4.1. Fundamental parameters of O-B-A stars

Early-type stars that do not show intrinsic emission lines in their spectrum and have not been detected as spectroscopic binaries are listed in Table 1, sorted by their EIS catalogue number. The fundamental parameters T_{eff} , $\log g$, $V \sin i$, and RV obtained by fitting the observed spectra, as well as the spectral classification deduced on one hand from $T_{\text{eff}} - \log g$ plane calibration (CFP determination, see Paper I) and on the other hand from equivalent width diagrams (CEW determination, see Paper I), are reported in Table 1. The heliocentric velocities (7 and 12 km s⁻¹) have been subtracted from the radial velocities.

To derive the luminosity, mass and radius of O, B, and A stars from their fundamental parameters, we interpolate in the HR-diagram grids (Schaller et al. 1992) calculated for the SMC metallicity ($Z = 0.001$; Maeder et al. 1999 and references therein) and for stars without rotation.

We estimate the mean radius, mean mass and mean $V \sin i$ in various mass bins (e.g. $5 < M < 7 M_{\odot}$, $7 < M < 9 M_{\odot}$, etc). We then obtain a mean equatorial velocity for a random angle distribution using formulae published in Chauville et al. (2001) and Paper I).

For B stars, $\langle V \sin i \rangle$ is close to 160 km s⁻¹, thus $V_e/V_c \simeq 43\%$ and $\Omega/\Omega_c \simeq 58\%$. As the effects of fast rotation on the spectra are only significant for $\Omega/\Omega_c > 60\%$ (Frémat et al. 2005), we do not need to correct the fundamental parameters of B stars for fast rotation effects. This justifies the use of non-rotating models. Although some B stars do have a high $V \sin i$ (> 350 km s⁻¹), the accuracy on the parameters determination is generally low for these stars, and thus we decide not to introduce corrections. Since the value of the averaged Ω/Ω_c is at the limit at which the spectroscopic effects of fast rotation appear, we however expect that a significant part of the B stars in the sample will be apparently more evolved due to gravitational darkening.

The obtained luminosity, mass, radius, and age of most O, B, and A stars of the sample are given in Table 2. The position of these stars in the HR diagram is shown in Fig. 2.

4.2. Fundamental parameters of Be stars

4.2.1. Apparent fundamental parameters

The sample (131 Be stars) includes 41 known Be stars from Keller et al. (1999) and from Grebel et al. (1992), for which the H α emissive character has been confirmed in this work,

Table 2. Parameters $\log(L/L_{\odot})$, M/M_{\odot} et R/R_{\odot} interpolated or calculated for our sample of O, B, A stars in the SMC from HR diagrams published in Schaller et al. (1992) for $Z=0.001$. The full table is available online.

Star	$\log(L/L_{\odot})$	M/M_{\odot}	R/R_{\odot}	age (Myers)
SMC5_000351	2.4 ± 0.4	3.4 ± 0.5	1.9 ± 0.3	125 ± 6
SMC5_000398	4.2 ± 0.4	9.7 ± 0.5	24.8 ± 2.5	26 ± 3
SMC5_000432	3.1 ± 0.4	4.5 ± 0.5	5.0 ± 1.0	119 ± 6
...

and 90 new Be stars. Three H α emission line stars mentioned in Keller et al. (1999) are not Be stars: the star SMC5_2807 or KWBB044 is a cool supergiant and a binary, the star SMC5_37102 or KWBB0485 is a possible HB[e], and the star SMC5_81994 or KWBB04154 is a planetary nebula.

The apparent fundamental parameters ($T_{\text{eff}}^{\text{app}}$, $\log g_{\text{app}}$, $V \sin i_{\text{app}}$, and RV) we derive for these stars are reported in Table 3. The spectral classification derived from apparent fundamental parameters is also given in the last column of the Table. Without correction for fast rotation nearly all Be stars seem to be sub-giants or giants.

The apparent luminosity, mass, radius, and age of Be stars are derived in the same way as for O, B and A stars (see Sect. 4.1), from their apparent fundamental parameters. The apparent position of Be stars in the H-R diagram is shown in Fig. 2 and the corresponding luminosities, masses, and radii are given in Table 4.

Table 4. Apparent parameters $\log(L/L_{\odot})$, M/M_{\odot} , and R/R_{\odot} interpolated or calculated for Be stars in the SMC from HR diagrams published in Schaller et al. (1992) for $Z=0.001$. The full table is available online.

Star	$\log(L/L_{\odot})$	M/M_{\odot}	R/R_{\odot}	age Myers
MHF[S9]47315	5.3 ± 0.4	23.9 ± 1.5	16.0 ± 1.5	7.6 ± 1
MHF[S9]51066	4.6 ± 0.4	13.1 ± 1.0	14.1 ± 1.5	16.2 ± 3
SMC5_000476	3.2 ± 0.4	5.2 ± 0.5	3.8 ± 0.5	77.2 ± 6
...

4.2.2. Fundamental parameters corrected for rapid rotation

The pnr fundamental parameters ($T_{\text{eff}}^{\text{pnr}}$, $\log g_{\text{pnr}}$, $V \sin i^{\text{true}}$) of Be stars we obtain after correction with FASTROT are given in Table 5 for different rotation rates Ω/Ω_c . We estimate the rotation rate Ω/Ω_c to be used for the selection of the most suitable pnr fundamental parameters of Be stars in the SMC as in Paper I. We obtain $V_e/V_c \simeq 87\%$ and $\Omega/\Omega_c \simeq 95\%$ on average.

As previously, but with the pnr fundamental parameters corresponding to the rotation rate $\Omega/\Omega_c = 95\%$, we derive the luminosity $\log(L/L_{\odot})$, mass M/M_{\odot} , and radius R/R_{\odot} for Be stars. These parameters are given in Table 6. After correction for rapid rotation, Be stars globally shift in the HR diagram towards lower luminosity and higher temperature, as illustrated

Table 1. Fundamental parameters for O, B, A stars in the SMC. The name, coordinates ($\alpha(2000)$, $\delta(2000)$), V magnitude and (B-V) colour index of stars are taken from the EIS catalogues. The effective temperature T_{eff} is given in K, $\log g$ in dex, $V \sin i$ in km s^{-1} and the RV in km s^{-1} . For each parameter the 1σ error is given. The abbreviation “CFP” is the spectral type and luminosity classification determined from fundamental parameters (method 2), whereas ‘CEW’ is the spectral type and luminosity classification determined from EW diagrams (method 1). The localization in clusters is indicated in the last column: cl0 for NGC 330 (0h 56m 19s -72° 27' 52"), cl1 for H86 170 (0h 56m 21s -72° 21' 12"), cl2 for [BS95]78 (0h 56m 04s -72° 20' 12"), cl3 for the association SMC ASS 39 (0h 56m 6s -72° 18' 00"), cl4 for OGLE-SMC109 (0h 57m 29.8s -72° 15' 51.9"), cl5 for NGC299 (0h 53m 24.5s -72° 11' 49") corrected coordinates, cl6 for NGC306 (0h 54m 15s -72° 14' 30"), cl7 for H86 145 (0h 53m 37s -72° 21' 00"), cl8 for OGLE-SMC99 (0h 54m 48.24s -72° 27' 57.8"). The full table is available online.

Star	$\alpha(2000)$	$\delta(2000)$	V	B-V	S/N	T_{eff}	$\log g$	$V \sin i$	RV	CFP	CEW	com.
SMC5_000351	00 53 32.810	-72 26 43.70	17.75	-0.15	20	16500±1600	4.4±0.2	312±47	158 ±10	B3V	B2.5IV	
SMC5_000398	00 54 02.700	-72 25 40.60	14.27	-0.12	90	13500±400	2.7±0.1	104±10	138 ±10	B5II-III	B0.5III	
SMC5_000432	00 53 19.101	-72 24 48.76	16.87	-0.14	60	15500±800	3.7±0.2	197±16	156 ±10	B3IV	B2III	
...

Table 3. See the caption of Table 1. In addition, MHF[SX]XXXXX is given for stars in our catalogue of emission line stars, and in the last column, the letter “k” followed by a number corresponds to the star number in Keller et al. (1999). Moreover the “#” indicates that the star was pre-selected in our catalogue of emission line stars (unpublished). In the last column the spectral classification from the SIMBAD database is also given. The last three lines correspond to emission-line objects which are not Be stars. The full table is available online.

Star	$\alpha(2000)$	$\delta(2000)$	V	B-V	S/N	$T_{\text{eff}}^{\text{app.}}$	$\log g_{\text{app.}}$	$V \sin i_{\text{app.}}$	RV	CFP	comm.
MHF[S61]47315	0 54 49.559	-72 24 22.35	-	-	120	30000±800	3.4±0.1	370±10	160±10	B0IV	#
MHF[S61]51066	0 54 50.936	-72 22 34.63	-	-	130	22500±600	3.3±0.1	415±10	130±10	B1III	#
SMC5_000476	0 53 23.700	-72 23 43.80	16.36	-0.15	40	18500±1400	4.0±0.2	309±30	110±10	B2V	
...

Table 5. Fundamental parameters for Be stars in the SMC corrected from the effects of fast rotation assuming different rotation rates (Ω/Ω_c). The most suitable corrections are those corresponding to $\Omega/\Omega_c=95\%$. The units are K for T_{eff}^o , dex for $\log g_o$, and km s^{-1} for $V \sin i^{\text{true}}$. The full table is available online.

star	$\Omega/\Omega_c=85\%$			$\Omega/\Omega_c=90\%$			$\Omega/\Omega_c=95\%$		
SMC	T_{eff}^o	$\log g_o$	$V \sin i^{\text{true}}$	T_{eff}^o	$\log g_o$	$V \sin i^{\text{true}}$	T_{eff}^o	$\log g_o$	$V \sin i^{\text{true}}$
MHF[S9]47315	33000 ±800	3.7 ±0.1	383 ±10	34000 ±800	3.7 ±0.1	390 ±10	32500 ±800	3.8 ±0.1	396 ±10
MHF[S9]51066	26500 ±600	3.7 ±0.1	428 ±10	27500 ±600	3.8 ±0.1	437 ±10	26000 ±600	3.8 ±0.1	450 ±10
SMC5_000476	20000 ±1400	4.3 ±0.2	321 ±30	20000 ±1400	4.3 ±0.2	328 ±30	20000 ±1400	4.3 ±0.2	336 ±30
...

in Fig.2. It clearly demonstrates that Be stars are less evolved than their apparent fundamental parameters could indicate.

Table 6. Parameters $\log(L/L_\odot)$, M/M_\odot , R/R_\odot and age of Be stars in the SMC, obtained by interpolation in the evolutionary tracks published in Schaller et al. (1992) with $Z=0.001$ with fundamental parameters corrected for fast rotation effects with $\Omega/\Omega_c=95\%$. The full table is available online.

Star	$\log(L/L_\odot)$	M/M_\odot	R/R_\odot	age Myears
MHF[S9]47315	5.0 ± 0.4	21.3 ± 1.5	10.2 ± 1.5	7.9 ± 1
MHF[S9]51066	4.4 ± 0.4	12.0 ± 1.0	7.6 ± 1.5	17.49 ± 3
SMC5_000476	3.0 ± 0.4	5.0 ± 0.5	2.5 ± 0.5	51.42 ± 6
...

4.2.3. Spectral lines saturation

According to Townsend et al. (2004) and Frémat et al. (2005, Figs. 5 and 6), there may be a saturation effect of the FWHM of spectral lines for the highest angular velocities (Ω/Ω_c) that hampers the estimate of $V \sin i$. However, the magnitude of this effect strongly depends on stellar parameters and on the studied line-transitions. Multiple line fitting, as we perform in our study, allows therefore to reduce the impact of the saturation (due to the gravitational darkening) and to correct it with FASTROT. This is confirmed by the fact that, for the SMC, we report apparent $\frac{V_c}{V_c}$ ratios which are significantly above the expected limit where saturation should appear (i.e. ~ 0.80).

4.3. Characteristics of the sample

To characterize the sample of stars, we study the distribution in spectral types, luminosity classes, and masses for stars in clusters and in the field. Note that the method with equivalent widths (CEW) fails to give a reliable spectral classification for

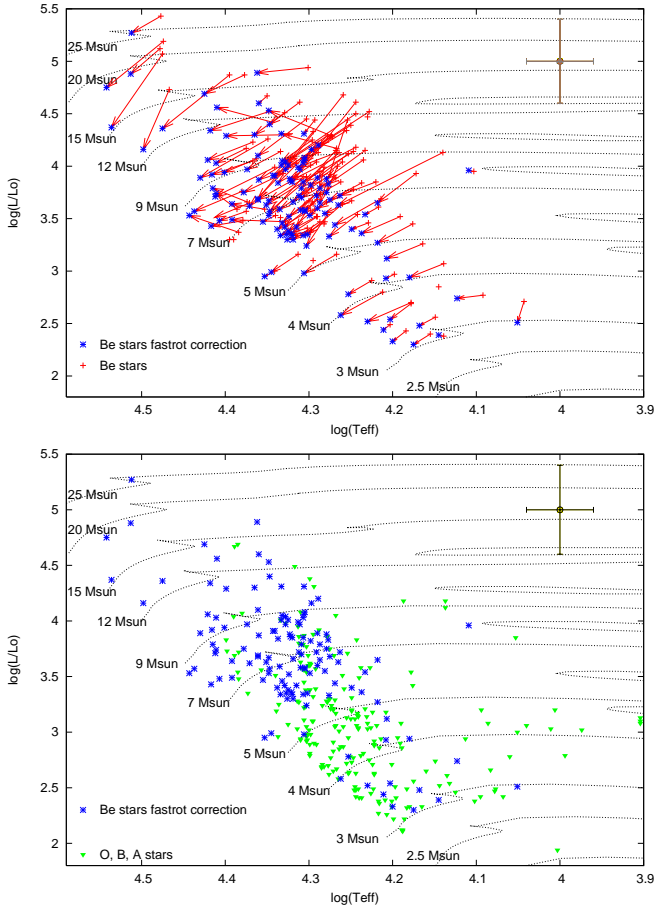


Fig. 2. HR diagrams for the studied B and Be stars. Top: The effects of fast rotation are taken into account with $\Omega/\Omega_c = 95\%$ for Be stars. Bottom: B stars and fast rotators (Be stars) corrected for their fast rotation. Common: The adopted metallicity for the SMC is $Z=0.001$. Red '+' represent Be stars with their apparent parameters, blue '*' Be stars corrected with FASTROT with $\Omega/\Omega_c = 95\%$, and green triangles B stars. Typical error bars are shown in the upper right corner of the figure. Evolutionary tracks come from Schaller et al. (1992).

the few hotter (late O) and cooler (B5-A0) stars in the sample. Moreover, for Be stars, the spectral classification determination is only performed using the derived apparent fundamental parameters (CFP), since the emission contamination, often present in H γ and in several cases in the He I 4471 line, makes the first method particularly inappropriate for early Be stars.

4.3.1. Distributions in spectral types and luminosity classes

We present in Fig. 3 the distribution of O-B-A stars with respect to spectral type and luminosity class. The classification used here is the one obtained from the fundamental parameters determination (CFP determination).

The sample contains essentially early B-type stars (B0 to B3) as in the LMC (Paper I) which are mainly dwarfs and subgiants (classes V, IV), in the field as well as in clusters.

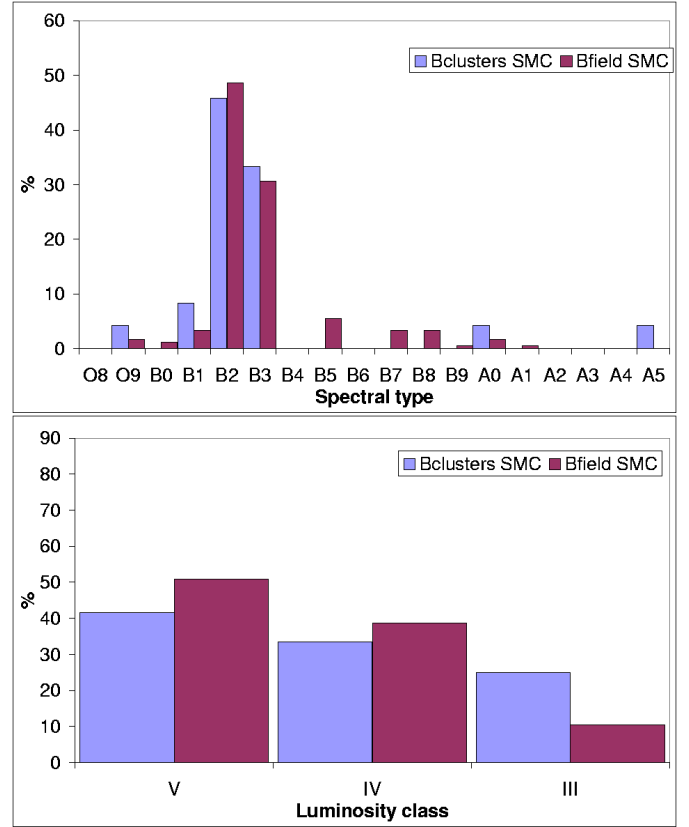


Fig. 3. Spectral type (upper panel) and luminosity class (lower panel) distributions of B-type stars in the sample in the SMC. In common: the blue left bars are for stars in clusters and the red right bars are for stars in fields.

We also present the distribution of Be stars with respect to luminosity class and spectral type, using the classification obtained from the fundamental parameters. We compare the distribution obtained before and after correction of fast rotation effects (Figs. 4 and 5).

As for B stars, Be stars in our sample generally are early B-type stars (B0 to B3) but are apparently giants and subgiants (classes III, IV). The Be stars corrected for rotation effects appear hotter than apparent fundamental parameters would suggest. In particular, there are more B1-type stars. After fast rotation treatment Be stars in classes III and IV are redistributed in classes IV and V. However, about 60% of the Be stars still appear as giants and subgiants as in the LMC (Paper I).

4.3.2. Distribution in masses

In addition, we investigate the mass distribution of B and Be stars (Fig. 6). The sample shows a distribution peaking around 5-6 and 7-8 M_\odot for B and Be stars, respectively. These peaks are reminiscent of those of B and Be stars in LMC's sample (7 and 10 M_\odot) as shown in Paper I, but are shifted to smaller masses.

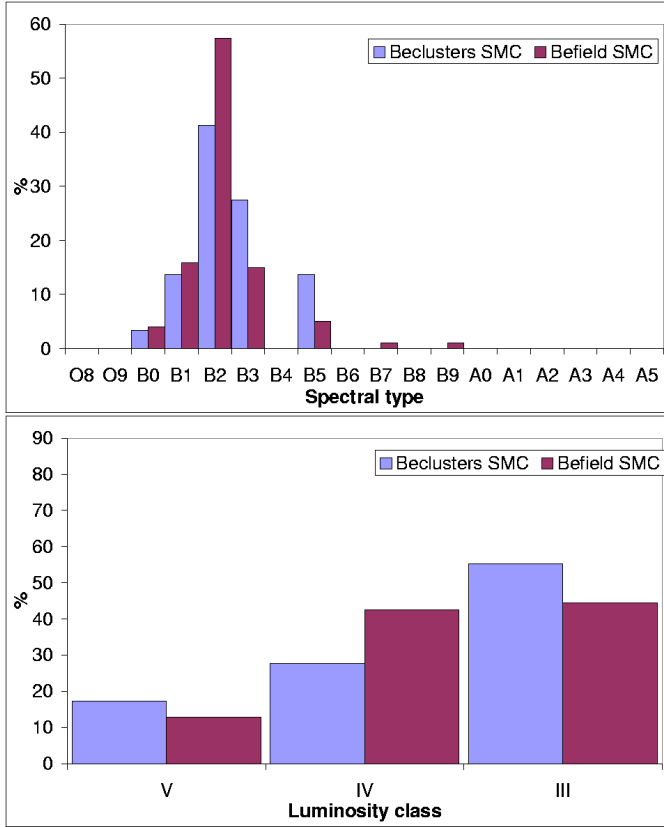


Fig. 4. Apparent spectral type (upper panel) and luminosity class (lower panel) distributions of Be stars in the sample in the SMC. In common: The blue left bars are for stars in clusters and the red right bars are for stars in fields.

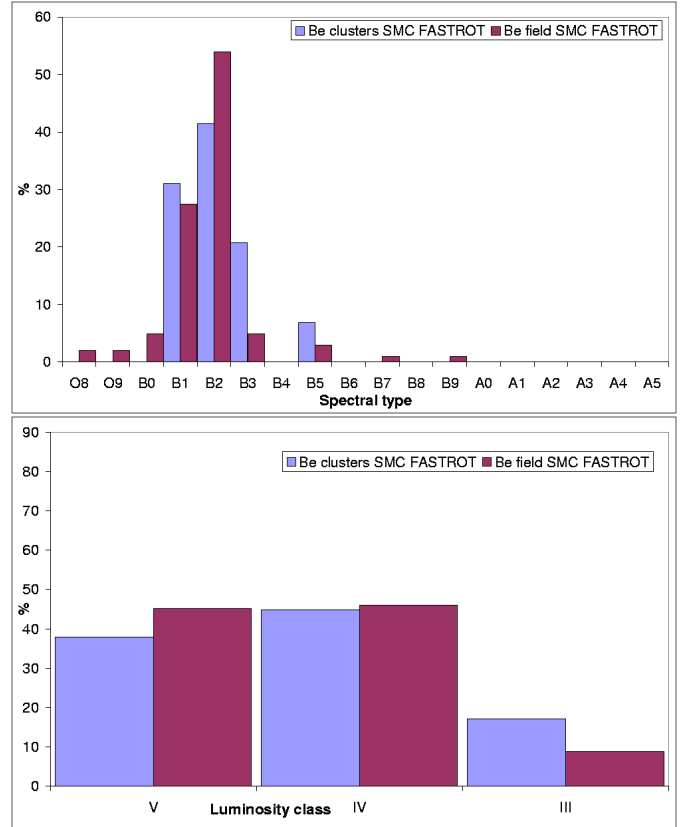


Fig. 5. Corrected spectral type (upper panel) and luminosity class (lower panel) distributions of Be stars after fast rotation treatment in the sample in the SMC. In common: The blue left bars are for stars in clusters and the red right bars are for stars in fields.

4.3.3. Ages of clusters

We determine the ages of stars of the field and of several clusters or associations in our observations. For this purpose, we use HR evolutionary tracks (for non-rotating stars) for the stars of the sample unaffected by rapid rotation and for Be stars corrected for the effects of fast rotation with $\Omega/\Omega_c = 95\%$. For the cluster NGC 330, we obtain $\log(t) = 7.5 \pm 0.2$, which is in excellent agreement with the value found photometrically by OGLE: 7.5 ± 0.1 (see Pietrzyński & Udalski 1999) while Chiosi et al. (2006) found $\log(t) = 8.0$. For the clusters OGLE-SMC99 and OGLE-SMC109, we find $\log(t) = 7.8 \pm 0.2$ and $\log(t) = 7.9 \pm 0.2$ to be compared with $\log(t) = 7.6 \pm 0.2$ and $\log(t) = 7.7 \pm 0.1$, respectively (Pietrzyński & Udalski 1999), with 7.3 and 7.4 respectively from Chiosi et al. (2006), and with 8.1 and 7.8 respectively from Rafelski & Zaritsky (2005) for a metallicity $Z=0.001$. In the same way, we determine the age of other clusters: for NGC299 $\log(t) = 7.8 \pm 0.2$ and NGC306 $\log(t) = 7.9 \pm 0.2$ to be compared with the values from Rafelski & Zaritsky (2005): 7.9 and 8.5 respectively. Our values are thus in general in good agreement with OGLE and other determinations. As for the LMC, these comparisons validate our method to determine ages for clusters.

5. Rotational velocity and metallicity: results and discussion

We compare the $V \sin i$ values obtained for B and Be stars in the SMC to those obtained for the LMC (Paper I) and given in the literature for the MW. However, the latter generally did not take fast rotation effects into account in the determination of fundamental parameters. Therefore, to allow the comparison with the MW, we report on the apparent rotational velocity in the case of rapid rotators in the SMC and LMC.

5.1. $V \sin i$ for the SMC in comparison with the LMC and MW

For the same reasons as in Paper I, we cannot directly compare the mean $V \sin i$ values of the sample in the SMC with values in the LMC and in the MW, because they are affected by ages and evolution, mass function of samples, etc. We must therefore select B and Be stars in the same range of spectral types and luminosity classes or of masses (when they are known) and ages for samples in the SMC, LMC, and MW.

To investigate the effect of metallicity and age on the rotational velocity, we first compare the mean $V \sin i$ of B and Be stars either in the field or in clusters in the SMC to the ones in the LMC and MW. Then, we compare the rotational veloc-

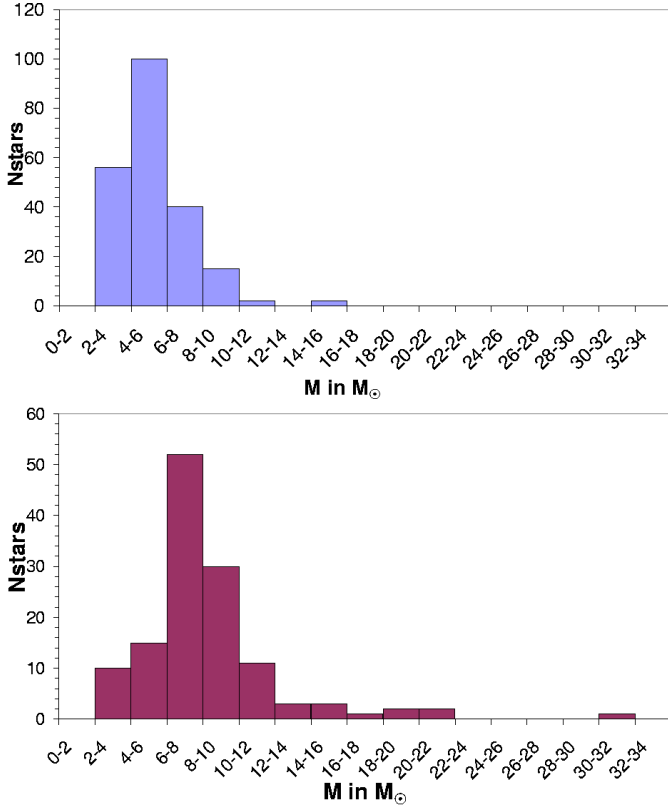


Fig. 6. Mass distribution of B (upper panel) and apparent mass distribution of Be stars (lower panel) in the sample in the SMC.

ity of B and Be stars in field versus clusters in the SMC. We use the same selection criteria as those for the LMC and MW described in Paper I: we select stars with spectral type ranging from B1 to B3 and luminosity classes from V to III. For reference studies in the LMC and MW, we use the same as those mentioned in Paper I (see Table 10 therein). The values are reported in Table 7. As in Paper I, we recall that all suspected binaries, shown in Martayan et al. (2005b) are removed from the statistics of the following sections.

5.1.1. Field B and Be stars

The comparison of $V \sin i$ in the SMC, the LMC and the MW for B and Be stars in the field are presented in Table 7 and Fig. 7 (upper panel). In the figure the range of stellar ages is reported as the dispersion in age. For samples with an unknown age, we adopt as error bar the duration of the main sequence for a $7 M_{\odot}$ star, which highly overestimates the age uncertainty. The curves show the evolutionary tracks of rotational velocity during the main sequence for different initial velocities for a $7 M_{\odot}$ star, which corresponds to the maximum of the mass function of the B-star sample. These curves are obtained as described in Paper I (Sect. 5.2).

As for the LMC, we show that the samples in the SMC contain a sufficient number of elements for the statistics to be relevant and give an average $V \sin i$ not biased by inclination effects. We complete the statistical study by the Student's t-test (Table online) in order to know whether the differences

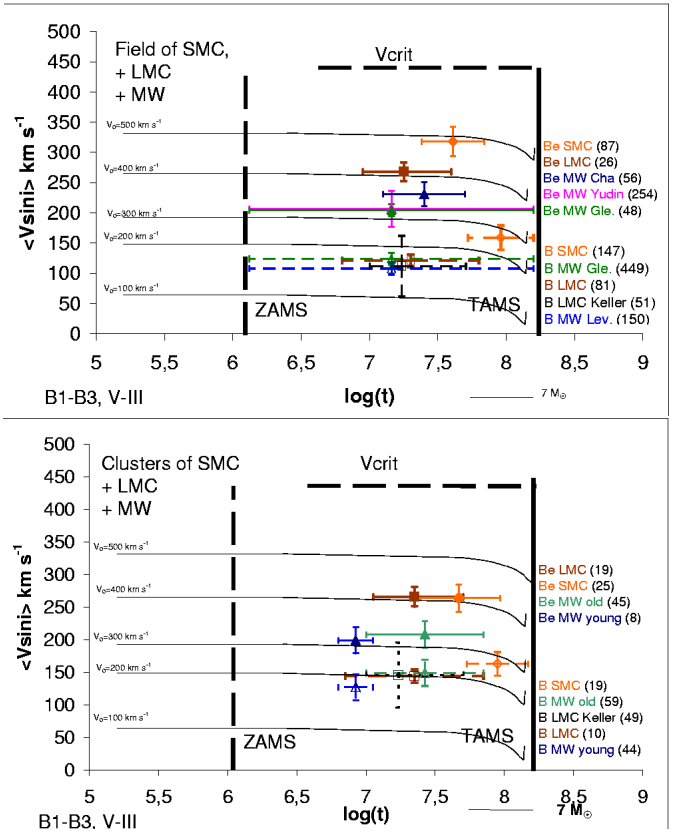


Fig. 7. Comparison of mean $V \sin i$ in the SMC, in the LMC and in the MW. Evolutionary tracks of rotational velocity during the main sequence life are given for different initial velocities for a $7 M_{\odot}$ star. The ZAMS and TAMS are indicated by vertical lines and the critical $V \sin i$ by a horizontal dotted line. The number of stars for each study is given in brackets. The dispersion in ages corresponds to the range of individual stellar ages in the samples, when these ages are known, or to the main sequence lifetime. Upper panel: for field B and Be stars. The considered studies are: for the SMC, this paper; for the LMC, Martayan et al. (2006b) and Keller (2004); for the MW, Cha = Chauville et al. (2001), Yudin (2001), Gle = Glebocki & Stawikowski (2000), and Lev = Levato & Grosso (2004). Lower panel: Same figure but for clusters. The considered studies are: for the SMC, this paper; for the LMC, Paper I and Keller (2004), and for the clusters in the MW, the WEBDA database.

observed between samples in the SMC, LMC and MW are significant.

(i) for field B stars: we find that there is a significant difference between the SMC, the LMC, and the MW. Field B stars in the SMC have a rotational velocity higher than in the LMC and the MW. We recall that the test is not conclusive between B stars in the LMC and the MW (Paper I), because results are different according to the selected study in the MW (Glebocki et al. 2000 or Levato et al. 2004).

(ii) for field Be stars: there is a slight difference between the SMC and the LMC, and a significant difference between the SMC and the MW. Field Be stars in the SMC have a higher rotational velocity than in the LMC and the MW. We also recall

Table 7. Comparison of mean rotational velocities for B and Be stars with spectral types B1-B3 and luminosity classes from V to III in the SMC, LMC and MW. The values in brackets represent the number of stars in the samples.

From		Field B stars	Field Be stars	Clusters B stars	Clusters Be stars
this study	SMC	159 ± 20 (147)	318 ± 30 (87)	163 ± 18 (19)	264 ± 30 (25)
Paper I	LMC	121 ± 10 (81)	268 ± 30 (26)	144 ± 20 (10)	266 ± 30 (19)
Paper I	LMC Keller (2004)	112 ± 50 (51)		146 ± 50 (49)	
Paper I	MW Glebocki et al. (2000)	124 ± 10 (449)	204 ± 20 (48)		
Paper I	MW Levato et al. (2004)	108 ± 10 (150)			
Paper I	MW Yudin (2001)		207 ± 30 (254)		
Paper I	MW Chauville et al. (2001)		231 ± 20 (56)		
Paper I	MW WEBDA $\log(t) < 7$			127 ± 20 (44)	199 ± 20 (8)
Paper I	MW WEBDA $\log(t) \geq 7$			149 ± 20 (59)	208 ± 20 (45)

that, from Paper I, field Be stars in the LMC have a rotational velocity higher than in the MW.

5.1.2. B and Be stars in clusters

The comparison of $V \sin i$ in the SMC, LMC and MW for B and Be stars in clusters are presented in Table 7 and Fig. 7 (lower panel). The evolutionary tracks curves are the same as in the upper panel. For the MW, we use the selection we made in Paper I. We distinguish two groups: the younger clusters with $\log(t) < 7$ and older clusters with $\log(t) \geq 7$. The age-difference between clusters, taken from WEBDA, gives the age-dispersion reported in the figure. The results concerning B and Be stars in the SMC, LMC and MW clusters are:

- (i) B stars in the SMC and LMC clusters seem to have a similar rotational velocity, as in the MW when interval of similar ages are compared (Paper I).
- (ii) for Be stars: We note no difference between Be stars in the SMC and LMC clusters, while there is a significant difference between the LMC and the MW clusters. Be stars rotate more rapidly in the Magellanic Clouds (MC) clusters than the MW clusters. The lack of difference between the SMC and the LMC is probably due to a difference in mass and evolution functions of the stars in the samples (see Section 4.3.2 and Paper I, Sect. 4.5.3).

5.1.3. Comparison between field and clusters

No significant differences can be found between rotational velocities neither for field versus cluster B stars in the SMC, LMC, and MW, nor for field versus cluster Be stars in the LMC and the MW. However, a slight trend seems to be present for Be stars in the SMC. Field Be stars seem to rotate faster than cluster Be stars in the SMC. However, note the large error bar on the mean $V \sin i$ value for Be stars in the SMC, which prevents conclusive results between field and clusters.

5.2. B and Be stars: mass and rotation

The search for links between metallicity and rotation of B and Be stars is also carried out thanks to a selection by masses, which allow a direct comparison with theoretical tracks of the rotational velocities. To obtain sub-samples in the most homo-

geneous possible way, we select the stars by mass categories: $5 \leq M < 10 M_{\odot}$, $10 \leq M < 12 M_{\odot}$, etc. We assume a random distribution for the inclination angle.

The number of observed stars for a given mass category is low, therefore we have not separated the stars in clusters and in fields categories. This is justified since we have not found any significant difference between the rotational velocities of stars in fields and in clusters. We first present a general result between B and Be stars in the MC, then we study in detail the effects of metallicity and evolution on the rotational velocities for Be stars in the MW and in the MC.

The rotational velocities we derived from observational results, for the different samples by mass categories for B and Be stars in the MC are reported in Fig. 8. This graph shows, as from spectral type-selection, that Be stars reach the main sequence with high rotational velocities at the ZAMS contrary to B stars. Consequently, only a B star with a sufficiently high initial rotational velocity at the ZAMS may become a Be star.

5.2.1. Effect of metallicity on B stars

The values of the mean rotational velocities for the mass-samples of B stars in the SMC and LMC are given in Table 9 and reported in Fig. 8. For a better comparison, we must reduce the number of degrees of freedom, i.e. compare the samples with similar ages and similar masses and with a sufficient number of elements. That is the case, in this study, for the 5-10 M_{\odot} category sample. Even if the age is not exactly the same, the evolution of the rotational velocity as shown by the tracks for a 7 M_{\odot} , indicate that the velocity of the SMC's sample is higher than the one of the LMC at exactly the same age. A highly significant difference (probability 99.5%) in the mean rotational velocity is then shown for this mass-category between the SMC and the LMC with the Student's t-test. Note that such a comparison cannot be done with B stars in the MW, because the data in the literature do not allow to determine their masses.

The effect of metallicity on rotational velocities for B stars is shown for the 5-10 M_{\odot} category with similar ages between the SMC and the LMC: the lower the metallicity, the higher the rotational velocities of B stars. It could also be valid for other ranges of masses, but this has to be confirmed with appropriate samples. Nevertheless, this observational result nicely confirms

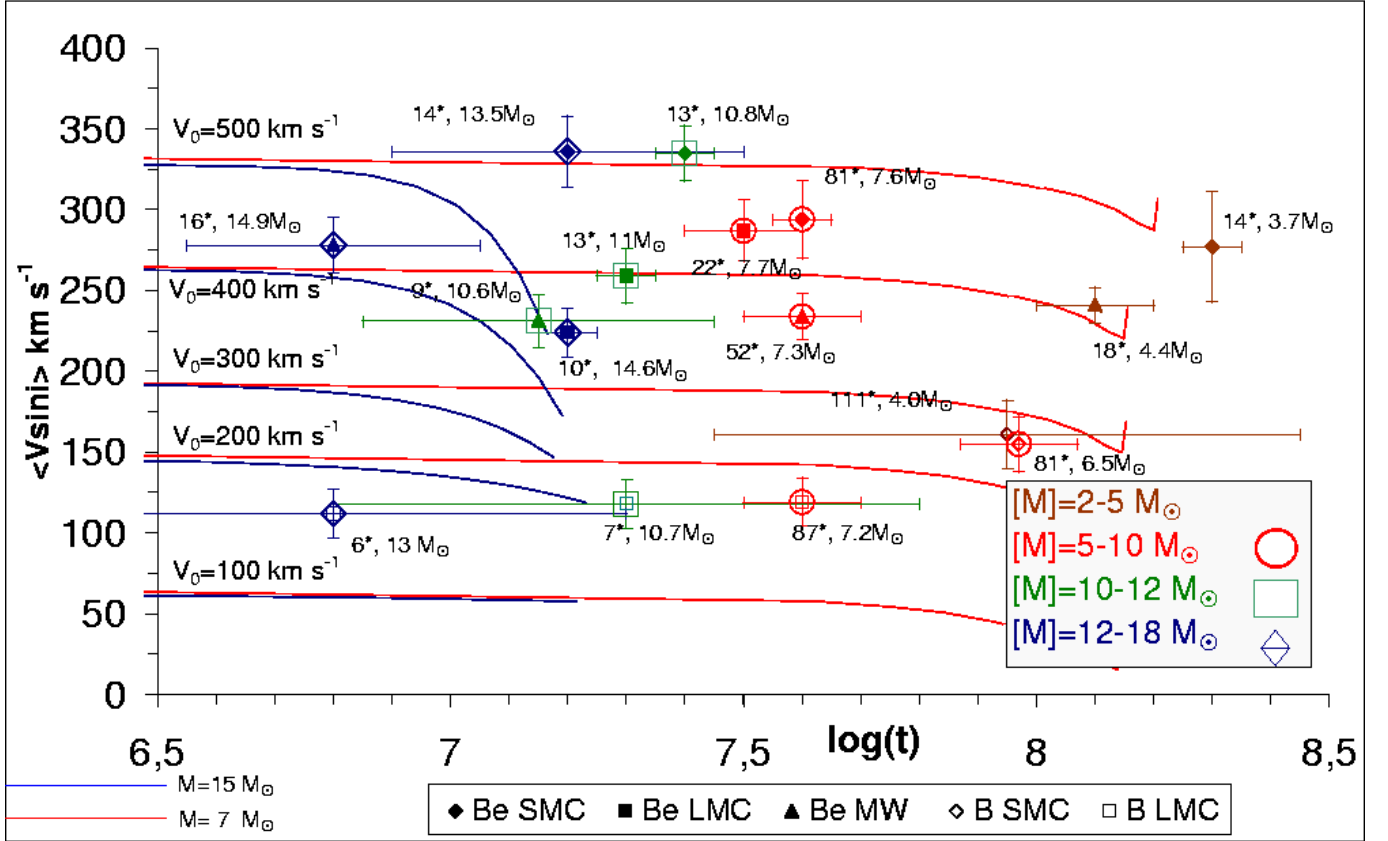


Fig. 8. Comparison of the rotational velocities for Be stars in the SMC, in the LMC and in the MW; and for B stars in the SMC and the LMC. The squares are for the samples of stars in the LMC, the diamonds are for the samples of stars in the SMC, and the triangles are for the samples of stars in the MW. Empty symbols are for the B stars, and full symbols are for Be stars. The different mass-categories are indicated by different colours and symbols which surround the symbols for the B and Be stars in the 3 galaxies: brown for masses ranging from 2 to 5 M_{\odot} , red large circles for masses ranging from 5 to 10 M_{\odot} , green large squares for masses ranging from 10 to 12 M_{\odot} , and blue large diamonds for masses ranging from 12 to 18 M_{\odot} . The numbers indicated next to each point correspond to the number of stars N^* in each sample and to their mean mass. The tracks of rotational velocities for a 7 and a 15 M_{\odot} star obtained for the SMC from our interpolations in the studies of Meynet & Maeder (2000, 2002), Maeder & Meynet (2001) are shown to illustrate the results.

Table 9. Comparison by mass sub-samples of the mean rotational velocities in the SMC and LMC B stars. For each sub-sample, the mean age, mean mass, mean $V \sin i$ and the number of stars (N^*) are given. No result is given for massive stars in the SMC, because of their small number.

	2-5 M_{\odot}				5-10 M_{\odot}			
	<age>	<M/ M_{\odot} >	<V sin i >	N^*	<age>	<M/ M_{\odot} >	<V sin i >	N^*
SMC B stars	8.0	4.0	161 \pm 20	111	8.0	6.5	155 \pm 17	81
LMC B stars	7.9	4.1	144 \pm 13	6	7.6	7.2	119 \pm 11	87
	10-12 M_{\odot}				12-18 M_{\odot}			
	<age>	<M/ M_{\odot} >	<V sin i >	N^*	<age>	<M/ M_{\odot} >	<V sin i >	N^*
SMC B stars				3				2
LMC B stars	7.3	10.7	118 \pm 10	7	6.8	13.0	112 \pm 10	6

the theoretical result of Meynet & Maeder (2000) and Maeder & Meynet (2001).

5.2.2. Effect of metallicity on Be stars

The selection by mass samples of Be stars in the SMC was done as in Paper I for the LMC. For the MW, we use the studies published by Chauville et al. (2001) and Zorec et al. (2005). The mean rotational velocity for each mass sample of Be stars is reported in Table 10 and is shown in Fig. 8 for the three

Table 10. Comparison by mass sub-samples of the mean rotational velocities for the samples of Be stars in the SMC, LMC and in the MW. For each sample, the mean age, the mean mass, the mean rotational velocity and the number of stars are given. Note no low-mass Be star in the LMC.

	2-5 M_{\odot}				5-10 M_{\odot}			
	<age>	<M/ M_{\odot} >	<V sin i >	N*	<age>	<M/ M_{\odot} >	<V sin i >	N*
SMC Be stars	8.0	3.7	277 \pm 34	14	7.6	7.6	297 \pm 25	81
LMC Be stars				0	7.5	7.7	285 \pm 20	21
MW Be stars	8.1	4.4	241 \pm 11	18	7.6	7.3	234 \pm 14	52
	10-12 M_{\odot}				12-18 M_{\odot}			
	<age>	<M/ M_{\odot} >	<V sin i >	N*	<age>	<M/ M_{\odot} >	<V sin i >	N*
SMC Be stars	7.4	10.8	335 \pm 20	13	7.2	13.5	336 \pm 40	14
LMC Be stars	7.3	11	259 \pm 20	13	7.2	14.6	224 \pm 30	10
MW Be stars	7.2	10.6	231 \pm 16	9	6.8	14.9	278 \pm 10	17

galaxies. For each sample, the mean age and mass, as well as the number of considered stars are given.

From the results of the Student's t-test in Table online, we conclude that there is an effect of metallicity on the rotational velocities for Be stars in samples with similar masses and similar ages: the lower the metallicity, the higher the rotational velocities. This is particularly visible in high-mass (10-12 M_{\odot}) and intermediate-mass (5-10 M_{\odot}) samples of Be stars in the SMC and the MW.

Note, moreover, that for the most massive-star samples (12 $\leq M < 18 M_{\odot}$), it is more difficult to compare them directly, since the ages are quite different between the MC and MW. We note the lack of massive Be stars in the MW at ages for which Be stars are found in the MC. It suggests that the Be star phase can last longer in low metallicity environments such as the MC, compared to the MW.

5.3. ZAMS rotational velocities of Be stars

The interpretation of our results requires a set of rotational velocity tracks for masses between 2 and 20 M_{\odot} , for different metallicities corresponding to the MC and the MW, and for different initial rotational velocities at the ZAMS. We obtain these tracks by interpolation in the models of the Geneva group as described in Sect. 5.3.1. For the first time we derive the distributions of the ZAMS rotational velocities of Be stars as shown in Sect. 5.3.2.

5.3.1. Theoretical evolutionary tracks of the rotational velocity

We derive rotational velocity evolutionary tracks for different masses, initial velocities and metallicities by interpolation in curves published by Meynet & Maeder (2000, 2002), Maeder & Meynet (2001). We proceed as reported in Paper I (Section 5.2) for a 7 M_{\odot} star. We then obtain curves for 3, 5, 7, 9, 12, 15, and 20 M_{\odot} stars, for initial rotational velocities $V_0=100, 200, 300, 400, 500 \text{ km s}^{-1}$, and at available metallicities $Z=0.020$ (solar metallicity), $Z=0.004$ (LMC), and $Z=0.00001$ (metallicity similar to the one of the first generation of stars). For $Z=0.001$ (SMC), the curves result from our interpolations. The

increase in the lifetime of stars on the main sequence due to rotation and metallicity is taken into account.

Note that due to fast internal angular momentum redistribution in the first $\approx 10^4$ years in the ZAMS, the surface rotational velocities decrease by 0.8 to 0.9 times their initial value. Moreover, for the comparison-sake with our observational data, the values plotted are not V but are averaged $V \sin i = (\pi/4)V$. For example, for an initial rotational velocity equals to 300 km s^{-1} , the angular momentum redistribution leads roughly to $V_{\text{ZAMS}} = 240 \text{ km s}^{-1}$, which corresponds to $V \sin i = (\pi/4) \times 240 \approx 190 \text{ km s}^{-1}$.

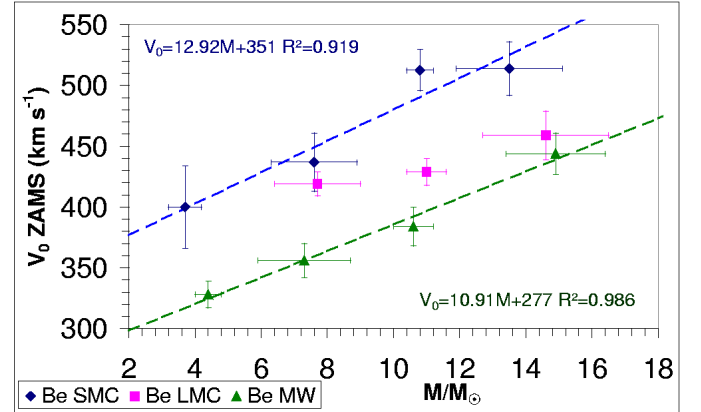


Fig. 9. ZAMS rotational velocities for the samples of Be stars in the SMC (blue diamonds), in the LMC (pink squares) and in the MW (green triangles). The dashed lines correspond to the linear regressions. Their corresponding equations and correlation coefficient are given in the upper left and lower right corners.

5.3.2. ZAMS rotational velocities

Our study shows that Be stars begin their life on the main sequence with higher rotational velocities than those for B stars. For each sample of Be stars in the SMC, LMC and MW, the initial rotational velocity at the ZAMS has been obtained by interpolation between the tracks of the evolution of rotational velocity during the MS (see Sect. 5.3.1). The resulting distribu-

tions of ZAMS rotational velocities for the samples of Be stars in the SMC, LMC and MW are shown in Fig. 9.

The average rotational velocities at the ZAMS (V_O) are quantified by linear regressions and their equations are as follows:

- In the SMC, $V_O = 12.92 \frac{M}{M_\odot} + 351$ and the correlation coefficient is $R^2=0.919$.
- In the MW, $V_O = 10.91 \frac{M}{M_\odot} + 277$ and the correlation coefficient is $R^2=0.986$.
- For the LMC, the lack of low mass stars in our sample implies that we cannot determine the ZAMS distribution. The later seems to be situated between the distributions of the SMC and MW.

5.3.3. Consequences

- Whatever the metallicity, the ZAMS rotational velocities of Be stars depend on their masses.
- Following the SMC and MW curves, the trend (the gradient) of the ZAMS rotational velocities of Be stars could be independent of the metallicity.
- There is an effect of metallicity on the distributions of the ZAMS rotational velocities. The lower the metallicity, the higher the ZAMS rotational velocities.
- There is a limit of the ZAMS rotational velocities below which B stars will never become Be stars. This limit depends on the metallicity.

The initial conditions (magnetic field, accretion disk, etc) in an open cluster will lead to a more or less high number of B stars with a ZAMS rotational velocity high enough to become Be stars. Therefore, the rates of Be stars will fluctuate depending on the cluster. It is expected that the mean rate of Be stars at low metallicity, typically in the SMC, is higher than at high metallicity, typically in the MW. This trend was already observed by Maeder et al. (1999) in open clusters. We find a similar result between the fields in the LMC and the SMC (Martayan et al. 2006c, in preparation). All these observational results give new constraints on the pre-main sequence (PMS) evolution of B and Be stars progenitors and, in particular, support the arguments exposed by Stepién (2002) about the influence of a magnetic field on formation conditions of B and Be stars (see Paper I, Sect. 5.2.5). Progenitors of Be stars would possess a weak magnetic field with a surface intensity between 40 and 400 G and, due to the short PMS phase for the early types, would conserve their strong rotational velocity during the main sequence. In low metallicity environments, the magnetic field has less braking impact, which could explain why Be stars in the SMC can rotate initially with higher velocities than in the LMC, and Be stars in the LMC with higher velocities than in the MW, as shown in Figs. 7 and 8. Note that a weak magnetic field is suspected in the classical Be star ω Ori (Neiner et al. 2003).

6. Angular velocity and metallicity: results and discussion

Thanks to the formulae published in Chauville et al. (2001) and in Paper I, it is possible to obtain the average ratio of angular to the breakup angular velocity for the stars.

6.1. Angular velocities for B stars

We determine the mean Ω/Ω_c ratio of B-type stars in the LMC (37%) and in the SMC (58%). In the same way, we determine this ratio in the MW with the values in Table 7; this ratio ranges from 30 to 40%.

The values of Ω/Ω_c seem to be similar for B stars in the MW and in the LMC, but higher in the SMC. This difference is probably due to the large difference of metallicity between the SMC and the LMC/MW. We recall that the considered stars in the MC have similar ages.

6.2. Angular velocities for Be stars

According to Porter (1996), the mean Ω/Ω_c ratio of Be-type stars in the MW is 84% in good agreement with the one (83%) determined by Chauville et al. (2001). Following the detailed study by Cranmer (2005) on Be stars in the MW, the ratio Ω/Ω_c ranges from 69% to 96% for the early-types. In the LMC (Paper I) this ratio ranges from 73% to 85%, and in the SMC (this study) from 94% to 100%. We recall that, in the MC, the observed Be stars are also early-types and have similar ages. We thus note the following trend: in the SMC they rotate faster than in the LMC/MW and are close to the breakup velocity or are critical rotators. This shows that, in a low metallicity environment such as the SMC, more massive Be stars can reach the critical velocity. We also note that Be stars appear with at least $\Omega/\Omega_c \approx 70\%$ in the LMC. This value seems to be a threshold value to obtain a Be star in the MW, LMC, and by extension certainly in the SMC.

According to the stellar wind theories and Maeder & Meynet (2001), the higher the mass of the star, the higher the mass loss and angular momentum loss. However, in low metallicity environments, this mass loss and consequently the angular momentum loss are lower than in the MW. As during the main sequence the radius of the star increases and as the star conserves high rotational velocities with a mass which decreases only slightly, the critical velocity decreases. Consequently, the Ω/Ω_c ratio for massive stars increases at low metallicity, while it decreases in the MW. For intermediate and low mass Be stars, whatever the metallicity, the Ω/Ω_c ratio first stays relatively constant and then increases at the end of the main sequence.

6.3. ZAMS angular velocities for Be stars

Thanks to the distributions of ZAMS rotational velocities for Be stars presented in Sect. 5.3 and with the mass, and radius at the ZAMS from the Geneva models, it is possible to obtain the ZAMS angular velocities and the Ω/Ω_c ratio for Be stars in the MW and in the MC. The results are given in Table 12. The

effect of metallicity on the angular velocities is visible at the ZAMS. Note that the ratio Ω/Ω_c increases as the mass of the star increases.

All the theoretical calculations from Meynet & Maeder (2000, 2002) and Maeder & Meynet (2001) have been performed with a ZAMS rotational velocity equal to 300 km s^{-1} . From the observations, we find that Be stars begin their MS lifetime with ZAMS rotational velocities higher than 300 km s^{-1} . For example, for a $20 M_\odot$ Be star, the ZAMS rotational velocity is equal to 495 km s^{-1} in the MW and 609 km s^{-1} in the SMC. The ZAMS rotation rate for a B star in the SMC is thus higher than the value adopted by Meynet & Maeder in their studies. In the SMC, it is consequently easier than expected for Be stars to reach the critical velocity. Note that, due to differential rotation, these stars could be critical rotators at their surface but not inside their core.

Table 12. Ratio of angular velocity to the breakup angular velocity Ω/Ω_c (%) at the ZAMS for Be stars in the MW and in the SMC (this study) for a 5, 12, $20 M_\odot$ star.

	MW	SMC
$5M_\odot \Omega/\Omega_c(\%)$	75	77
$12M_\odot \Omega/\Omega_c(\%)$	80	84
$20M_\odot \Omega/\Omega_c(\%)$	85	92

7. Evolutionary status of Be stars

7.1. Observational results for Be stars in the SMC

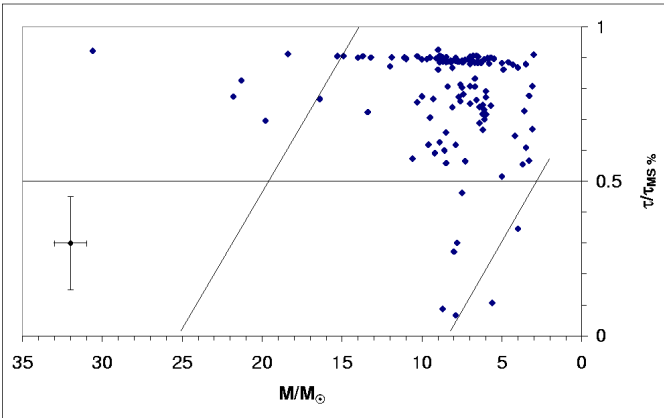


Fig. 10. Evolutionary status of Be stars in the SMC. The fast rotation effects are taken into account with $\Omega/\Omega_c=95\%$. The typical errors are shown in the lower left corner. The diagonals show the area of existing Be stars in the MW (Zorec et al. 2005).

To investigate the evolutionary status of Be stars in the SMC taking into account the effects of fast rotation and the low metallicity ($Z=0.001$) of the SMC, we firstly calculate the lifetime of the main sequence (τ_{MS}) of massive stars by interpolation in grids of evolutionary tracks provided by Maeder

& Meynet (2001) and Meynet & Maeder (2000) for different metallicities, with an initial velocity $V_0 = 300 \text{ km s}^{-1}$ and for stars with masses higher than $9 M_\odot$. Secondly, we extrapolate the τ_{MS} values towards lower masses ($5-9 M_\odot$). We then investigate the evolutionary status $\frac{\tau}{\tau_{MS}}$ of the SMC Be stars using the values of their ages corrected from fast rotation effects and given in Table 6. Results are shown in Fig. 10.

The following remarks can be made:

- It appears that more massive Be stars in the SMC are evolved: all of them in our sample are localized in the second part of the MS.
- Intermediate mass Be stars are scattered across the MS.
- Less massive Be stars are mainly evolved and in the second part of the MS ($\frac{\tau}{\tau_{MS}} \geq 0.5$).

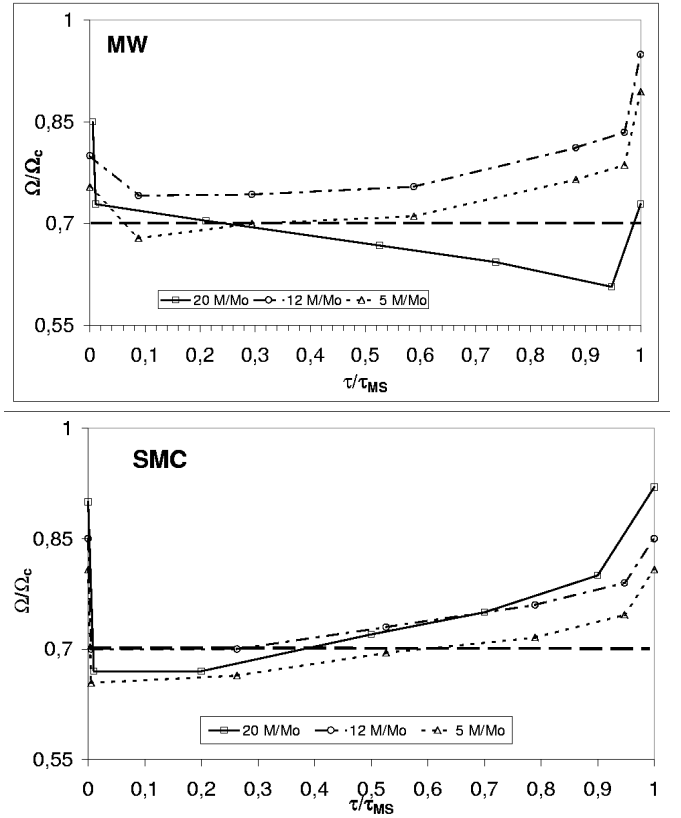


Fig. 11. Evolution of the Ω/Ω_c ratio for 3 types of stars: $20 M_\odot$ (squares), $12 M_\odot$ (circles) and $5 M_\odot$ (triangles) stars in the MW (top) and in the SMC (bottom). The stars may become Be stars if $\Omega/\Omega_c \geq 70\%$ (noted with a long dashed line).

7.2. Comparison between the evolutionary status of Be stars in the MC and MW

To compare the evolutionary status of Be stars in the different galaxies we calculate the $\frac{\tau}{\tau_{MS}}$ ratio for massive and less massive stars in the LMC ($Z=0.004$) and the MW (solar metallicity) as for the SMC. We note that in the MW, our results are quite similar to the ones in Zorec et al. (2005). However, in the LMC, our

Table 13. Proportions in SMC, LMC, and MW of Be stars (in %) in the upper ($\frac{\tau}{\tau_{MS}} > 0.5$) and lower ($\frac{\tau}{\tau_{MS}} \leq 0.5$) MS for masses $> 12 M_{\odot}$ and $\leq 12 M_{\odot}$. The values for the MW are taken from Zorec et al. (2005).

$M > 12 M_{\odot}$			
	MW	LMC	SMC
$\frac{\tau}{\tau_{MS}} > 0.5$	30	100	100
$\frac{\tau}{\tau_{MS}} \leq 0.5$	70	0	0
$M \leq 12 M_{\odot}$			
	MW	LMC	SMC
$\frac{\tau}{\tau_{MS}} > 0.5$	65	77	94
$\frac{\tau}{\tau_{MS}} \leq 0.5$	35	23	6

previous results shown in Paper I (Fig. 12) are slightly modified with the use of evolutionary tracks adapted to its metallicity ($Z=0.004$), mainly for the less massive Be stars which appear more evolved in the present study. The proportions of more massive ($>12 M_{\odot}$) and less massive ($\leq 12 M_{\odot}$) Be stars in the SMC, LMC and MW are summarized in Table 13. It is shown that all more massive stars in the LMC and the SMC are in the upper part of the MS ($\frac{\tau}{\tau_{MS}} \geq 0.5$), contrary to the MW where they are mainly in the lower part of the MS. The less massive stars seem to follow the same trend in the MW and the MC, they are mainly in the upper part of the MS in agreement with Fabregat & Torrejón (2000). With our results on the ZAMS rotational velocity distributions (Fig. 9) and with the theoretical evolution of angular velocities taken from the Geneva models mentioned above, we obtain the evolution of the angular velocities for different masses (5, 12, 20 M_{\odot}) of Be stars in the MW and the SMC as it is shown in Fig. 11. We have emphasized significant behaviour differences between Be stars in function of their mass and of their metallicity environment, and we propose the following explanation of the Be phenomenon in the MW and in the MC:

- More massive Be stars:

In the MW, more massive stars begin their life in the MS with a high Ω/Ω_c ($>70\%$, see Fig. 9 and Table 12), thus these stars could be Be stars. Then, by angular momentum loss, the stars spin down and might not eject matter anymore; thus, they lose their “Be star” character during the first part of the MS (typically for $\frac{\tau}{\tau_{MS}} > 0.2$). However, at the end of the MS ($\frac{\tau}{\tau_{MS}} \simeq 1$), during the secondary contraction, massive stars could have Ω/Ω_c sufficiently high to become Be stars again.

In the MC, more massive stars begin their life in the MS with a high Ω/Ω_c ($>70\%$) and could be Be stars but only at the very beginning of the ZAMS. Therefore, they rapidly lose “the Be star status”. However, they spin up (increase of the radius, low mass-loss and low angular-momentum loss) and reach very high Ω/Ω_c at the end of the first part of the MS (typically after $\frac{\tau}{\tau_{MS}} > 0.4$) so that they become Be stars again, contrary to what is observed in the MW.

- Intermediate mass Be stars:

In the MW as in the MC, intermediate mass Be stars begin their life in the MS with high Ω/Ω_c ($>70\%$, Fig. 9

and Table 12), therefore the stars could be Be stars. Then, the evolution of their Ω/Ω_c allows these stars to remain Be stars.

- Less massive Be stars:

In the MW as in the MC, less massive stars begin their life on the MS with Ω/Ω_c sufficiently high to obtain the status of “Be stars”. After the fast internal angular redistribution in the first $\simeq 10^4$ years in the ZAMS, the surface rotational velocities decrease and the stars lose the status of “Be stars”. Then, the evolution of their Ω/Ω_c allows these stars to become Be stars again (typically after $\frac{\tau}{\tau_{MS}} > 0.5$), in agreement with Fabregat & Torrejón (2000).

We note that our propositions explain results presented by Zorec et al. (2005, their Fig. 6) and our results concerning the LMC (Paper I) and the SMC (Fig. 10). We also remark no difference between the evolutionary status of Be stars in clusters and fields.

In summary, a B star can become a Be star if its progenitor has a strong initial rotational velocity at the ZAMS. Depending on the metallicity of the environment of a star and on the stellar mass, the Be phenomenon appears at different stages of the MS.

8. Conclusions

With the VLT-GIRAFFE spectrograph, we obtained spectra of a large sample of B and Be stars in the SMC-NGC 330 and surrounding fields. We determined fundamental parameters for B stars in the sample, and apparent and parent non-rotating counterpart (pnrc) fundamental parameters for Be stars.

Using results from this study and those obtained for the LMC with the same instrumentation (Paper I), we made a statistical comparison of the behaviour of B and Be stars in the Magellanic Clouds with the MW.

- there is no difference in rotational velocities between early-type stars in clusters and in fields in the LMC and in the SMC.
- the lower the metallicity is, the higher the rotational velocities are. B and Be stars rotate faster in the SMC than in the LMC, and faster in the LMC than in the MW.
- we have determined, for the first time, the distributions of the ZAMS rotational velocities of Be stars. The ZAMS rotational velocities are mass-dependent and metallicity-dependent. The gradients of the distributions seem to be similar whatever the metallicity.
- Only a fraction of B stars, that reach the ZAMS with sufficiently high initial rotational velocities, can become Be stars. Wisniewski & Bjorkman (2006) seem to have found photometrically a similar result.
- the angular velocities are similar for B stars in the LMC and in the MW and lower than those in the SMC. The same result is obtained for Be stars.
- more massive Be stars in the SMC, which are evolved, are critical rotators.
- in an evolutionary scheme, massive Be stars in the MC and more particularly in the SMC appear in the second part of

the main sequence, to the contrary to massive Be stars in the MW, which appear in the first part of the main sequence.

- other categories of Be stars (intermediate and less massive Be stars) follow the same evolution whatever the metallicity of the environment.

Our results support Stepień's scenario (2002): massive stars with a weak or moderate magnetic field and with an accretion disk during at least 10% of their PMS lifetime would reach the ZAMS with sufficiently high initial rotational velocity to become Be stars.

Our observational results also support theoretical results by Meynet & Maeder (2000, 2002) and Maeder & Meynet (2001) for massive stars. In a more general way they illustrate the behaviour of massive stars and the importance of the processes linked to rotation and to metallicity. In particular, our results show that rotation has a major role in the behaviour of massive stars. Moreover, this pioneer study of a large sample of B stars in low metallicity environments, such as the LMC (Paper I) and the SMC (this study), allows us to approach the "first stars". We can reasonably expect that first massive stars are fast rotators.

In forthcoming papers, we will present results of CNO abundances determinations, discuss the proportion of Be stars and report on the discovery of binaries in the SMC.

Acknowledgements. We would like to thank Dr V. Hill for performing the observing run in September 2004 with success and good quality. We thank Drs C. Ledoux, P. François, and E. Depagne for their help during the observing run in October 2003. This research has made use of the Simbad database and VizieR database maintained at CDS, Strasbourg, France, as well as of the WEBDA database.

References

- Castelli, F., Gratton, R. G., & Kurucz, R. L. 1997, A&A, 318, 841
- Chauville, J., Zorec, J., Ballereau, D., et al. 2001, A&A, 378, 861
- Chiosi, E., Vallenari, A., Held, E. V., et al. 2006, A&A, 452, 179
- Cranmer, S. R. 2005, ApJ, 634, 585
- Fabregat, J., Torrejón, J. M. 2000, A&A, 357, 451
- Frémat, Y., Zorec, J., Hubert, A.-M., et al. 2005, A&A, 440, 305
- Frémat, Y., Neiner, C., Hubert, A.-M., et al. 2006, A&A, 451, 1053
- Glebocki R., Stawikowski A. 2000, Acta Astr., 50, 509
- Grebel, E. K., Richtler, T., de Boer, K. S. 1992, A&A, 254, L5
- Hubeny, I. & Lanz, T. 1995, ApJ, 439, 875
- Jasniewicz, G., Thévenin, F. 1994, A&A, 282, 717
- Keller, S. C., Wood, P. R., Bessell, M. S. 1999, A&ASS, 134, 489
- Keller, S. C. 2004, PASA, 21, 310
- Kurucz, R. L. 1993, Kurucz CE-ROM No.13. Cambridge, Mass.: Smithsonian Astrophysical Observatory.
- Levato, H. & Grosso, M. 2004, IAUS, 215, 51
- Martayan, C., Hubert, A.-M., Floquet, M., et al. 2005a, Active OB stars meeting, Sapporo Japan, 28/08-02/09/2005, S. Stefl, S. Owocki, A. Okazaki (eds), ASP Conf. Series, astroph0602149
- Martayan, C., Floquet, M., Hubert, A.-M., et al. 2005b, Active OB stars meeting, Sapporo Japan, 28/08-02/09/2005, S. Stefl, S. Owocki, A. Okazaki (eds), ASP Conf. Series, astroph0602148
- Martayan, C., Hubert, A.-M., Floquet, M., et al. 2006a, A&A, 445, 931 (M06)
- Martayan, C., Frémat, Y., Hubert, A.-M., et al. 2006b, A&A, 452, 273 (Paper I)
- Martayan, C., Floquet, M., Hubert, A.-M., et al. 2006c (in preparation) A&A
- Maeder, A., Grebel, E. K., Mermilliod, J.-C. 1999, A&A, 346, 459
- Maeder, A., Meynet, G. 2001, A&A, 373, 555
- Meynet, G., Maeder, A. 2000, A&A, 361, 101
- Meynet, G., Maeder, A. 2002, A&A, 390, 561
- Momany, Y., Vandame, B., Zaggia, S., et al. 2001, A&A, 379, 436
- Neiner, C., Hubert, A.-M., Frémat, Y., et al. 2003, A&A, 409, 275
- Pietrzyński, G., Udalski, A. 1999, Acta Astr., 49, 157
- Porter, J. M. 1996, MNRAS, 280, 31
- Rafelski, M. & Zaritsky, D. 2005, AJ, 129, 2701
- Schaller, G., Schaerer, D., Meynet, G., Maeder, A. 1992, A&AS, 96, 269
- Stepień, K. 2002, A&A, 383, 218
- Townsend, R. H. D., Owocki, S.P., Howarth, I.D. 2004, MNRAS, 350, 189
- Wisniewski, J.P. & Bjorkman, K.S. 2006, astroph0606525
- Yudin, R. V. 2001, A&A, 368, 912
- Zorec, J., Frémat, Y., Cidale, L. 2005, A&A, 441, 235

List of Objects

' ω Ori' on page 11